New role of TRPM4 channel in the cardiac excitation-contraction coupling in response to physiological and pathological hypertrophy in mouse

Christophe Hédon, Karen Lambert, Nourdine Chakouri, Jérôme Thireau, Franck Aimond, Cécile Cassan, Patrice Bideaux, Sylvain Richard, Adèle Faucherre, Jean-Yves Le Guennec, et al.

New role of TRPM4 channel in the cardiac excitation-contraction coupling in response to physiological and pathological hypertrophy in mouse

Christophe Hedon [a, 1], Karen Lambert [a, 1], Nourdine Chakouri [a], Jérôme Thireau [a], Franck Aimond [a], Cécile Cassan [a], Patrice Bideaux [a], Sylvain Richard [a], Adèle Faucherre [b], Jean-Yves Le Guennec [a], Marie Demion [a, *]

[a] PhyMedExp, Université de Montpellier, INSERM U1046, UMR CNRS, 9412, Montpellier, France
[b] IGF, Université de Montpellier, INSERM, CNRS, Montpellier, France

Keywords:
Myocardial infarction
Hypertrophy
TRPM4 channel
SOCE
Arrhythmias

A B S T R A C T

The transient receptor potential Melastatin 4 (TRPM4) channel is a calcium-activated non-selective cation channel expressed widely. In the heart, using a knock-out mouse model, the TRPM4 channel has been shown to be involved in multiple processes, including β-adrenergic regulation, cardiac conduction, action potential duration and hypertrophic adaptations. This channel was recently shown to be involved in stress-induced cardiac arrhythmias in a mouse model overexpressing TRPM4 in ventricular cardiomyocytes. However, the link between TRPM4 channel expression in ventricular cardiomyocytes, the hypertrophic response to stress and/or cellular arrhythmias has yet to be elucidated. In this present study, we induced pathological hypertrophy in response to myocardial infarction using a mouse model of *Trpm4* gene invalidation, and demonstrate that TRPM4 is essential for survival. We also demonstrate that the TRPM4 is required to activate both the Akt and Calcineurin pathways. Finally, using two hypertrophy models, either a physiological response to endurance training or a pathological response to myocardial infarction, we show that TRPM4 plays a role in regulating transient calcium amplitudes and leads to the development of cellular arrhythmias potentially in cooperation with the Sodium-calcium exchange (NCX).

Here, we report two functions of the TRPM4 channel: first its role in adaptive hypertrophy, and second its association with NCX could mediate transient calcium amplitudes which trigger cellular arrhythmias.

1. Introduction

The Transient Receptor Potential Melastatin 4 (TRPM4) member of the TRP channels superfamily is a calcium-activated non-selective cationic channel (NSC_{Ca}). Previously, we and others have reported its important role in cardiac physiology, including electrical conduction, arrhythmias, heart size and adaptive hypertrophy in mouse, human and rabbit models (Abriel et al., 2012; Gueffier et al., 2017; Guinamard et al., 2006a, 2014; Hof et al., 2013; Jacobs et al., 2015; Kruse et al., 2009; Liu et al., 2010; Mathar et al., 2010, 2014; Pironet et al., 2019; Simard et al., 2013; Uhl et al., 2014; Wang et al., 2013). In human, numerous mutations in the *TRPM4* gene, leading to a loss or a gain of function of the TRPM4 channel, are associated with inherited isolated cardiac conduction disorders, right bundle-branch block, tachycardia or Brugada syndrome (Duthoit et al., 2012; Kruse et al., 2009; Liu et al., 2010, 2013; Stallmeyer et al., 2012). The $Trpm4^{-/-}$ mouse model has been very useful for understanding the implication of the TRPM4 channel in many cardiac functions such as the β-adrenergic reserve and the hypertrophic response to Angiotensin II treatment or endurance training. More recently, an elegant study has evaluated the consequences of a gain-of-function in a mouse model by injecting AAV9 particles encoding TRPM4 (Pironet et al., 2019). These mice were more vulnerable to develop premature ventricular ectopic beats during exercise induced β-adrenergic stress.

* Corresponding author. Inserm U1046, Physiologie & Médecine Expérimentale du Cœur et des Muscles, 34 295, Montpellier, France.
E-mail address: marie.demion@inserm.fr (M. Demion).
[1] Both co-first authors.

The link between TRPM4 expression and cardiac hypertrophy or electrical disorders remains unclear. Regarding arrhythmias, TRPM4 has been implicated in atrial action potential duration as well as in transient inward currents (Iti) responsible for diastolic arrhythmias. This suggests a role for this channel in early and delayed after-depolarizations (Hu et al., 2017; Simard et al., 2012, 2013; Wang et al., 2013).

Concerning cardiac hypertrophic adaptation, it has been demonstrated that TRPM4 channels are involved in the shift between physiological and pathological hypertrophy by regulating the calcineurin-NFAT (Nuclear Factor of Activated T-lymphocytes) pathway. Indeed, by negatively regulating the store-operated calcium entry (SOCE), TRPM4 channels are able to inhibit calcineurin activation and thus the translocation of NFAT into the nucleus. In parallel, the decrease in calcineurin phosphatase activity allows the Akt pathway to be fully activated, which can in turn inhibit the calcineurin pathway (Dai et al., 2014; DeBosch et al., 2006; Kemi et al., 2008; Kim et al., 2008; Martin et al., 2012; Matsui et al., 2003; Oliveira et al., 2009; Wilkins et al., 2004).

In this study, we have tried to demonstrate how TRPM4 is able to link cellular arrhythmias and hypertrophic signaling pathways by using two types of cardiac hypertrophic remodeling: one physiological and one pathological.

Indeed, in a previous study, we have shown that TRPM4 channels are functionally expressed at the ventricular level and thus negatively regulate SOCE. We subsequently postulated that the SOCE inhibition favors the physiological versus the pathological signaling pathway by activating Akt and inhibiting the Calcineurin-NFAT pathway.

Here, we used a mouse model of myocardial infarction to induce a cellular pathological hypertrophic remodeling in order to i) validate the functional expression of the TRPM4 channel at the ventricular level in conditions of induced pathological cellular hypertrophy, ii) confirm the importance of TRPM4 for Akt and/or calcineurin signaling, and iii) understand the role TRPM4 plays in the regulation of excitation-contraction coupling.

2. Methods

2.1. Animals

Knock-out mice (*Trpm4*$^{-/-}$) and littermate controls (*Trpm4*$^{+/+}$) were obtained as previously described (Barbet et al., 2008; Demion et al., 2014). All procedures conformed to the Directive 2010/63/EU of the European Parliament and the Council of the September 22, 2010 on the protection of animals used for scientific purposes (agreement number: A34-172-38) and were approved by the "comité Ethique pour l'Expérimentation Animale - Région Languedoc-Roussillon" (protocol number: CEEA-LR-12110). Mice were housed in a pathogen free, controlled environment (21 ± 1 °C; 60% humidity; lights on from 08:00 a.m. to 8:00 p.m.; food and water available *ad libitum*; enriched environment) with 5 mice per cage, except for ECG experiments, where mice with telemetric device were isolated in individual cages for recordings.

We separated the mice (8 old weeks) into 2 groups: the "trained group", where physiological hypertrophy was induced, and the "surgical (myocardial infarction-MI) group", where pathological hypertrophy was induced with Sedentary and Sham mice as a control, respectively.

-*Surgical group*: The MI model was obtained by performing a ligature of the left coronary artery at 10 weeks of age under general anesthesia and mechanical ventilation. Briefly, the chest was opened by left lateral thoracotomy. The left coronary artery was isolated with surrounding myocardium using a 7–0 Prolene suture (Ethicon, Johnson and Johnson) with a tapered needle and the suture was tightened over the artery to induce ischemia and necrosis of the left ventricular anterior wall. The same protocol of anesthesia and surgery was used for the surgical control group (Sham) with thoracotomy and pericardial incision but without coronary ligature.

The cellular hypertrophy in the peri-infarct zone was assessed by measuring the cellular capacitance of isolated cardiomyocytes (see above for methods) which reflects the cell surface area (see supplementary Fig. 1).

-*Trained group*: all mice underwent 2 weeks of familiarization with treadmill and experimenter (15 min at 12 m/min, 5% slope, 5 days/week) and were then divided into 2 subgroups: sedentary mice and trained mice. The trained mice ran at 70% of their Maximal Aerobic Speed for 4 weeks for 1 h/day, 5 days/week, on a treadmill with a 5% slope (the hypertrophy was validated by the measurement of heart size using echocardiography in supplementary Fig. 2).

2.2. Echocardiography

Echocardiography analyses were performed using Vivid7Pro system (GE Healthcare, Chalfont St Giles, UK) equipped with a 14 MHz linear transducer (i13L, GE Healthcare) in conscious mice.

A two-dimensional view of the left ventricle (LV) was obtained at the level of the papillary muscles in a parasternal short-axis view. LV morphological parameters were measured from M-mode traces recorded through the anterior and posterior walls. The LV shortening fraction (LVSF) was calculated as [(LVIDd − LVIDs)/LVIDd x 100], where LVIDd and LVIDs are the end-diastolic and end-systolic Left Ventricle Internal Dimensions respectively. The LV mass (LVM) was calculated following the Devereux's formula: [(AWTd + LVIDd + PWTd)^3 − PWTd^3] x 1.04, where AWTd and PWTd are the anterior and posterior wall thickness of the LV in diastole respectively.

Echocardiograms were used for the validation of the PMI (we excluded mice without left ventricle remodeling) on one hand, and for the study of the morpho-functional adaptations on trained mice, on another hand (Gueffier et al., 2017).

2.3. Electrocardiograms (ECGs)

For long-term ECG recordings in conscious and unrestrained mice, telemetry devices (model TA10ETA-F20, Data Sciences International St. Paul, MN, USA) were implanted under general anesthesia (2% inhaled isoflurane in O2, Aerrane®, Baxter, France). ECGs were recorded using a telemetric receiver (model RPC-1) located below the animal cage and connected to a data acquisition system (IOX2, EMKA Technologies, Paris, France). Data were collected continuously over 24 h at 2 KHz. Recordings were digitally pass-filtered between 0.1 and 1000 Hz and analyzed off-line with the ECG-auto software, version 1.5.12.22 (EMKA Technologies). Twelve-hour nocturnal ECG signals were scanned by hand to detect, identify and count the absolute spontaneous rhythm disorders.

2.4. Enzymatic cells dissociation

Cardiac ventricular myocytes were enzymatically dissociated using standard procedures (Fauconnier et al., 2010). Succinctly, the mouse was euthanized by cervical dislocation, the heart was quickly excised and retrogradely perfused at 37 °C for 6–8 min with a modified Tyrode solution (in mM): NaCl 113, KCL 4.7, KH_2PO_4 0.6, Na_2HP_4 0.6, $MgSO_4$ 1.2, $NaHCO_3$ 12, $KHCO_3$ 10, HEPES 10, Taurine 30 (pH 7.4) containing 0.1 mg mL^{-1} of Liberase (Roche). Isolated myocytes were isolated from the free wall of the left ventricle after the resection of the scare and then transferred to the same enzyme-free solution containing 1 mM $CaCl_2$.

2.5. Cellular electrophysiology

Whole-cell patch-clamp recordings were performed (Axon Instruments, Foster City, CA) at room temperature (22–24 °C) to record cell membrane capacitance and AP on LV myocytes enzymatically isolated from *Trpm4*$^{+/+}$ and *Trpm4*$^{-/-}$ mice (Demion et al., 2014). The recording pipettes contained (in mM): KCl 120; EGTA 8; HEPES 10; $MgCl_2$ 6.8; $CaCl_2$ 3; $ATPNa_2$ 4; and $GTPNa_2$ 0.4 (pH 7.2). The bath solution contained (in mM): NaCl 130; KCl 4; $MgCl_2$ 1.8; $CaCl_2$ 1.8; HEPES 10; glucose 11 (pH 7.4). Cell capacitance was measured following brief voltage steps (±10 mV) from the holding potential to provide an estimation of cell size. The Ca^{2+} concentration in the pipette was estimated at 70 nM.

TRPM4-like current recording, after 5 mM caffeine application, were performed using the whole cell configuration of the patch-clamp technique using an Axopatch 200B (Axon instruments) as previously published (Gueffier et al., 2017; Köster et al., 1999). Patch electrodes had a DC resistance between 2 and 4 MΩ when filled with the different recording solutions. Currents were sampled at 2.5 kHz and filtered at 1 kHz. The protocol consisted on test pulses which were preceded by five depolarizing prepulses from −60 to +10 mV in order to load the SR with Ca^{2+}, followed by 5s pulse from −40 to 40 mV with 20 mV of $\Delta V_{m.}$ Data were analyzed using the pClamp 10.0 software (Molecular Devices Corporation).

The extracellular solution contained (mM): LiCl 140, $CaCl_2$ 1.8, $MgCl_2$ 1, 10 HEPES, glucose 10, tetraethylammonium chloride (TEA) 20; buffered at pH 7.4 with LiOH. pipette solution contained (mM): CsCl 140, TEA-Cl 20, $MgCl_2$ 1, HEPES 10 and EGTA 10, pH 7.2 with CsOH. The Ca^{2+} concentration in the pipette was adjusted at 60 nM by adding appropriate amounts of $CaCl_2$ (759 μM) calculated by the Maxchelator program (https://somapp.ucdmc.ucdavis.edu/pharmacology/bers/maxchelator/downloads.htm). Currents were measured in the whole-cell configuration.

To calculate the permeability ratio PCs^+/PLi^+ we used the modified Goldman-Hodgkin-Katz relation (Lee and Tsien, 1984).

$$\frac{PCs}{PLi} = \frac{([Li]out - [Li]in * e^{ErevF/RT}}{[Cs]in * e^{ErevF/RT} - [Cs]out}$$

Erev is the observed current reversal potential
Pion = permeability for that ion
[ion]out or in = the concentration for that ion outside or inside
R = the ideal gas constant in Joule per Kelvin per mole
F=Faraday's constant in Coulombs per mole
And T = Temperature in Kelvin

2.6. Western blot analysis

50 μg of total proteins from whole free wall of the LV were separated by 10% SDS-PAGE and were transferred onto nitrocellulose membranes (0.2 μm, GE Healthcare, Brumath, France). Protein expression was assessed by immunoblot analysis using anti-PhosphoSer473-Akt (P-Akt; #4060), anti-Akt (#9171), Pan-CalcineurinA (#2614), Pan 14-3-4 (#8312) (Cell Signaling, Ozyme, Montigny-le-Bretonneux, France), anti-TRPM4 (Abcam, St Aubin, France) and anti-GAPDH (PA1-913, Fisher Scientific, Illkirch, France) primary antibodies. All immunoblots were visualized and quantified using the Odyssey® infrared imaging system (LI-COR Biosciences, Lincoln, Nebraska, USA) coupled to infrared-labeled anti-goat, anti-mouse or anti-rabbit IgG secondary antibodies (1/30 000 dilution) (LI-COR Biosciences, Courtaboeuf, France). All primary and secondary antibodies were diluted in StartingBlock (TBS) blocking buffer.

2.7. PCR

Genomic PCR were performed on tail DNA with primers (Sigma-Aldrich) specific for the wild-type and null alleles (as described in (Barbet et al., 2008)). Total RNA was isolated from a minimum of 5 samples per group using the Nucleospin total mRNA isolation kit (Macherey-Nagel, Hoerdt, France) according to the manufacturer's instructions. Total mRNA, oligo-dT and random hexamer primers were used to generate cDNA using a Verso enzyme kit (Thermo-Fischer, Illkirch, France). RT-PCR for the evaluation of the expression of *Trpm4*, *Gapdh*, *BNP, Serca2a* and *ANF* were performed using gene-specific primers and performed in duplicate. Reactions were achieved using SYBR green Mix (Roche Applied System, Meylan, France) and commercially prepared primers (Sigma-Aldrich, Saint-Quentin Fallavier, France) (see primer sequences in (Gueffier et al., 2017).

For *Trpm4* gene expression comparison, we used the *Gapdh* gene as a housekeeping gene.

2.8. Store operated calcium entry (SOCE) measurement

Changes in intracellular Ca^{2+} concentration ($[Ca^{2+}]_i$) were determined in freshly isolated ventricular cardiomyocytes using the ratiometric fluorescent Ca^{2+} indicator Fura-2. Cells were plated on dishes and incubated with 2.5 μM Fura-2AM (Tef-labs) plus 0.02% pluronic acid F-127 (Molecular Probes Inc), in modified Tyrode solution (in mM: 145 NaCl, 5.4 KCl, 1 $MgCl_2$, 10 glucose, 10 N-(hydroxyethyl)piperazine-N′-2-ethanesulfonic acid (HEPES) and in 5 mM EGTA (pH 7.5 with NaOH)) during 30 min at 37 °C in a humidified air incubator. The cells were then washed with modified Tyrode solution containing 10 μM Nifedipine and 5 μM kB-R7943 buffer and mounted on the microscope stage at room temperature for 15 min to allow Fura-2AM de-esterification. Store depletion was induced by 5 mM of caffeine application. Measurements of the Fura-2 fluorescence at 510-nm were achieved from images digitally captured every second by a cooled CCD camera (Photometrics) with a ×20 objective lens mounted on an inverted microscope (Axiovert, Zeiss). Image acquisition was performed after excitations at 340- and 380-nm using a lambda-DG4 excitation system (Sutter Instrument Company, USA). Ca^{2+} signals were then analyzed by using the Metafluor software (Universal Imaging Corporation, USA). The results are given as the variation from basal values of the 340/380 nm recordings ratio after background correction.

2.9. Excitation-contraction coupling measurement

Real time Ca^{2+} imaging was performed on freshly isolated cardiomyocytes from left ventricle incubated in a physiological modified Tyrode solution (in mM): 140 NaCl, 4 KCl, 1 $MgCl_2$, 5 HEPES, 1.8 $CaCl_2$ and 11 glucose, (pH 7.4). Cardiomyocytes were loaded with the ratiometric Ca^{2+} dye Fura-2 AM (2 μmol/L, Life technologies, St-Aubin, France) and cell shortening/Ca^{2+} transients were simultaneously recorded using electrical-field stimulation (1 Hz). Sarcomere length (SL) and emitted fluorescence at 510-nm after a stimulation at 340 nm (F340) and 380 nm (F380) were simultaneously recorded using the IonOptix® system (Milton, USA) coupled to a Zeiss microscope (40*x* oil, 0.36 μm/pixel. When specified, β-Adrenergic receptors were stimulated by an incubation with isoproterenol (Iso) (10 nM) with or without the TRPM4 inhibitor 9-Phenanthrol (9-Phe) (10 μM). Cellular ectopic Ca^{2+} waves defined by any spontaneous rise of intracellular Ca^{2+} during the diastolic phase were considered as proarrhythmogenic cellular activity. In all experiments, at least 10 cells were recorded per

animal. Data were analyzed using the IonWizard 6.4 software.

2.10. Statistical analysis

Statistical analysis were performed using the GraphPad Prism software. All data are expressed as means ± standard error of the mean (SEM). N represents the number of mice and n the number of cells when indicated. For comparisons between *Trpm4*$^{+/+}$ and *Trpm4*$^{-/-}$ mice, a Mann-Whitney *U* test was performed. Comparison between survival rate of *Trpm4*$^{-/-}$ and *Trpm4*$^{+/+}$ PMI mice was performed using the Log-rank (Mantel Cox) test. *P*-values of 0.05 or less indicated a significant difference between groups. *P < 0.05; **P < 0.001; ***P < 0.0001; ns: no significant.

3. Results

3.1. TRPM4 is essential for survival after myocardial infarction

In order to determine the role of TRPM4 in pathological cellular hypertrophy, we induced a myocardial infarction (MI) in 10-week-old knock-out (*Trpm4*$^{-/-}$) and littermate control (*Trpm4*$^{+/+}$) mice. After 4 weeks, unlike previous study (Jacobs et al., 2015), the survival rate was significantly reduced in the MI-*Trpm4*$^{-/-}$ group (10/24 death) when compared to the MI-*Trpm4*$^{+/+}$ group (1/13 death) (n = 13 and 24 mice respectively (P = 0.0081); Fig. 1A). Cardiac function was assessed by echocardiography at 28 days post-surgery on MI and sham operated mice from both the *Trpm4*$^{+/+}$ and *Trpm4*$^{-/-}$ strains. The left ventricle fractional shortening (LVFS) was significantly reduced in the MI mice when compared to the sham mice in both strains and this reduction was even more pronounced in the MI-*Trpm4*$^{-/-}$ mice (Fig. 1B and supplementary Tables 1 and 2).

We next performed echocardiograms (Supplementary Tables 1 and 2) ~~(ECG)~~ from which we calculated the LV mass (LV mass corrected with Devereux's Formula). The hypertrophy observed between sham mice (2.628 ± 0.017 and 3.168 ± 0.16 mg/g in *Trpm4*$^{+/+}$ and *Trpm4*$^{-/-}$mice, respectively, P = 0.0203), was amplified in MI mice (2.499 ± 0.25 and 3.855 ± 0.41 mg/g in *Trpm4*$^{+/+}$ and *Trpm4*$^{-/-}$ mice, respectively, P < 0.01).

ECGs were also recorded for 12 h during the night in order to count spontaneous rhythm disorders. Although sham-*Trpm4*$^{-/-}$ mice displayed significantly more premature ventricular contractions (PVC) than the sham-*Trpm4*$^{+/+}$(as previously described in (Demion et al., 2014), after 4 weeks, the myocardial infarction induced an increase in the PVC occurrence in MI-*Trpm4*$^{-/-}$ when compared to MI-*Trpm4*$^{+/+}$ mice (Fig. 1C), while no modification of the heart rate was observed (data not shown). To assess whether these arrhythmias were dependent on cellular sensitivity, we isolated ventricular cardiomyocytes and recorded the membrane potential. After an electrical stimulation of 2Hz for 2 min, cells underwent an electrical quiescent period, in order to count early and delayed after depolarizations (EADs and DADs, respectively). In accordance with our ECG data, cells isolated from sham-*Trpm4*$^{-/-}$ mice triggered DADs as well as EADs and cells isolated from MI-*Trpm4*$^{-/-}$ mice also displayed more EADs and DADs than MI-*Trpm4*$^{+/+}$ mice (Fig. 1D–E).

Altogether, these data suggest that TRPM4 is essential for survival after a myocardial infarction. Indeed, the absence of the channel lead to a decrease in the ejection fraction and was associated with cellular and ventricle arrhythmias.

3.2. TRPM4 expression is upregulated after myocardial infarction and regulates store operated calcium entry

To study TRPM4 expression after myocardial infarction, we first performed quantitative RT-PCR on extracted hearts. *Trpm4* mRNA level was significantly increased in MI-*Trpm4*$^{+/+}$ when compared to sham-*Trpm4*$^{+/+}$ ventricles, while no mRNA was detected in KO ventricles (sham and MI mice) (Fig. 2A). We next assessed TRPM4 protein levels by Western blot. The protein was only detected in total protein extracts from MI-*Trpm4*$^{+/+}$ mice (Fig. 2B).

To validate the functionality of increased TRPM4 expression, we performed patch-clamp experiments using the whole cell configuration. In freshly isolated cardiomyocytes, TRPM4-like currents were observed after 5 mM caffeine application (Fig. 2C). Indeed, the TRPM4 channel is a calcium activated protein and, in our conditions, the TRPM4 current was due to cesium and lithium ions. The reversal potential observed for the caffein-induced current was −38mV, indicating a P_{Cs}/P_{Li} of 4. This is consistent with the permeability sequence described for TRPM4 channels (Nilius et al., 2005) where K^+>Na^+>Cs^+>Li^+ (Fig. 2C).

As the TRPM4 channel is known to regulate Ca^{2+} entry, we next analyzed the Ca^{2+} levels in cardiomyocytes from sham and MI *Trpm4*$^{+/+}$ and *Trpm4*$^{-/-}$ mice after application of caffeine (5 mM). No significant difference in Ca^{2+} release from internal stores was observed among the different conditions (Fig. 2D and E, left histograms). To determine whether Ca^{2+} entry could be regulated differently, we added 1 mM Ca^{2+} 90 s later. Indeed, we found that the amplitude of the fluorescent signal was proportional to the number of store-operated channels opened by sarcoplasmic calcium depletion following caffeine application. We observed a significant decrease of Ca^{2+} entry in cardiomyocytes freshly isolated from MI-*Trpm4*$^{+/+}$ when compared to sham-*Trpm4*$^{+/+}$, while no difference was observed between cells isolated from sham and MI *Trpm4*$^{-/-}$ mice. This result suggests that TRPM4 is able to reduce store-operated Ca^{2+} entry (Fig. 2D and E, right histograms).

3.3. Cardiac hypertrophy induced by MI is associated with cellular pathological markers

In a previous study, we have shown that TRPM4 was able to maintain the balance between physiological and pathological hypertrophy following endurance training (Gueffier et al., 2017). We subsequently sought to determine whether pathological markers could also be affected by TRPM4 after MI by measuring P-Akt (activated during physiological hypertrophy), Calcineurin A (activated under pathological conditions) and the 14.3.3 protein chaperone (a protein involved in TRPM4 expression at the plasma membrane) protein levels. We observed that these pathways were indeed also activated in MI ventricles when compared to sham ventricles in *Trpm4*$^{+/+}$ mice, while no difference was observed between sham- and MI- *Trpm4*$^{-/-}$ mice (Fig. 3A). RT-PCR analysis of pathological hypertrophic markers, such as increased *BNP* and *ANF* expression or decreased *Serca2a* expression, revealed no difference between extracts from *Trpm4*$^{+/+}$ and *Trpm4*$^{-/-}$ ventricles (Fig. 3B). This indicates that pathological hypertrophy is triggered in both strains and that TRPM4 is required to regulate the signaling pathways involved in the cell size regulation.

3.4. TRPM4 is involved in the regulation of calcium transients following β-adrenergic stimulation

TRPM4 is a calcium activated channel which in turn regulates calcium entry. Because calcium signals are differentially regulated depending on their source, we investigated whether TRPM4 is involved in the regulation of calcium transients during excitation-contraction coupling (ECC). TRPM4 is functionally expressed in both our models of cellular hypertrophy: physiological, induced in response to endurance training, and pathological (see Supplementary Figure 2), induced in the border zone after MI (see

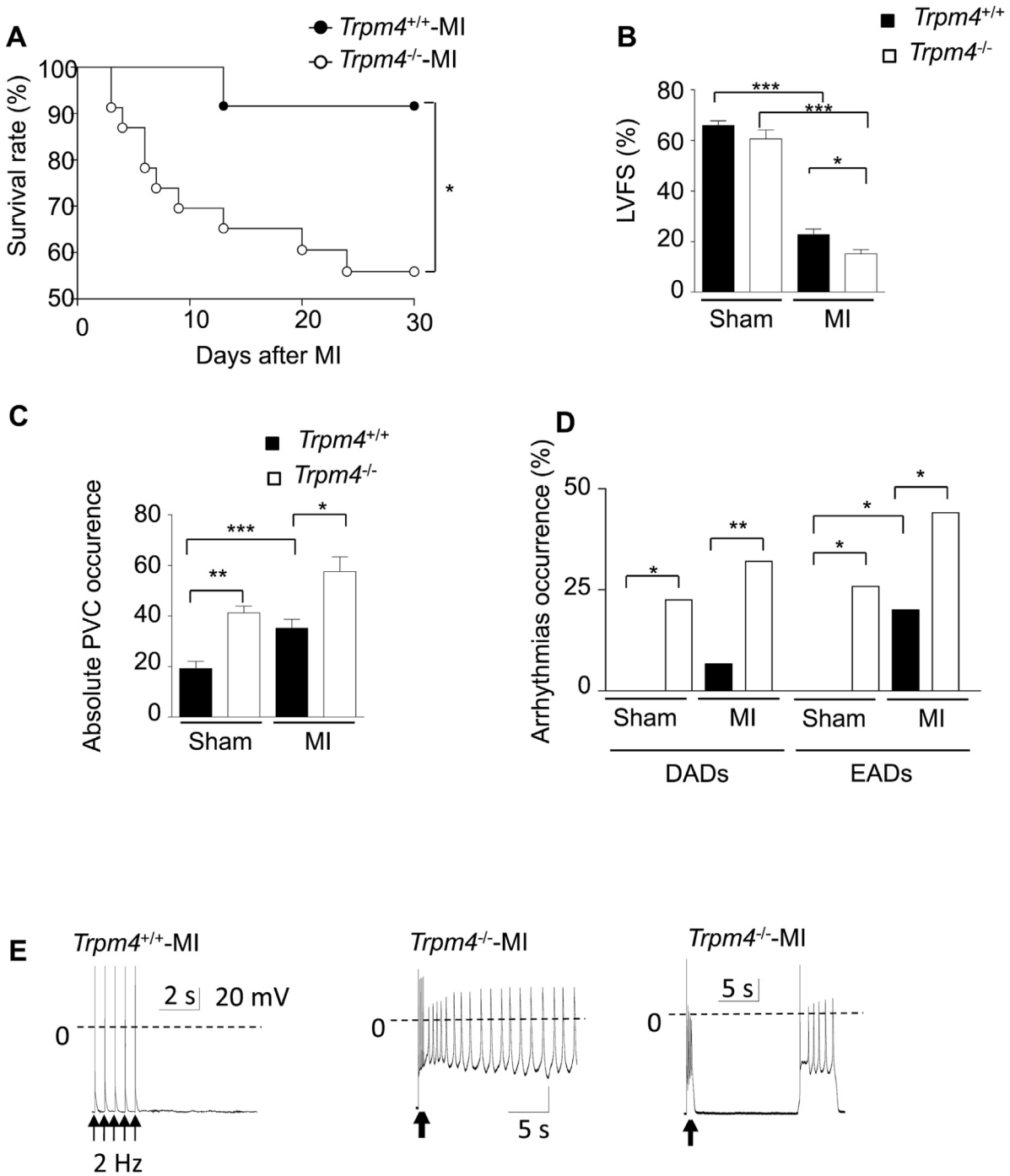

Fig. 1. PMI-*Trpm4*$^{-/-}$ mice display a decreased survival rate associated with ventricular arrhythmias. **A.** Kaplan-Meier Survival analysis in MI-*Trpm4*$^{+/+}$ (black circles) and MI-*Trpm4*$^{-/-}$ (white circles) mice after myocardial infarction (N = 13 and N = 24, respectively). **B.** Left ventricle fractional shortening (LVFS) assessed by echocardiography in vigils sham-*Trpm4*$^{+/+}$ (N = 12), MI-*Trpm4*$^{+/+}$ (N = 13), sham-*Trpm4*$^{-/-}$ (N = 16) and MI- *Trpm4*$^{-/-}$ (N = 12) mice. **C.** Absolute Premature ventricular contractions (PVC) analysis on 12h ECG recordings in vigils sham- *Trpm4*$^{+/+}$ (N = 5), MI-*Trpm4*$^{+/+}$ (N = 7), sham-*Trpm4*$^{-/-}$ (N = 10) and MI- *Trpm4*$^{-/-}$ (N = 9) mice. **D.** Arrhythmia occurrence analysis (%) of early (EAD) and delayed after-depolarization (DAD) using the current clamp technique in freshly isolated left ventricular myocytes after 10s of electrical stimulation (1Hz) (sham- *Trpm4*$^{+/+}$ (0/13 cells displayed DAD and 0/13 cells displayed EAD), MI-*Trpm4*$^{+/+}$ (2/28 cells displayed DAD and 8/31 cells displayed EAD), sham-*Trpm4*$^{-/-}$ (7/31 cells displayed DAD and 8/31 cells displayed EAD) and MI- *Trpm4*$^{-/-}$ (8/25 cells displayed DAD and 11/25 cells displayed EAD) mice. **E.** Illustration of membrane potential recording. Black arrows represent the electrical stimulation. Middle panel illustrates EAD, while right panel illustrates EAD and then DAD. N stands for the number of animals. Data are presented as mean ± SEM in B and C, statistical analysis were performed as mentioned in methods section *P < 0.05; **P < 0.01; ***P < 0.001.

Supplementary Figure 1). To investigate whether TRPM4 expression could influence ECC, we recorded calcium transients in freshly isolated cardiomyocytes from sham, MI, sedentary (Sed) and trained (Tr) mice. To decipher the implication of TRPM4, we used a specific blocker, 9-Phenanthrol (9-Phe, 10 μM), in order to inhibit the channel activity during the calcium transient measurement. In cardiomyocytes from sham-*Trpm4*$^{+/+}$ mice, 9-Phe application did not modify the diastolic Ca^{2+} level or the Ca^{2+} transient amplitude, correlating with the fact that we did not observe expression of TRPM4 in these mice (Fig. 4A–C and Fig. 2B). However, 9-Phe

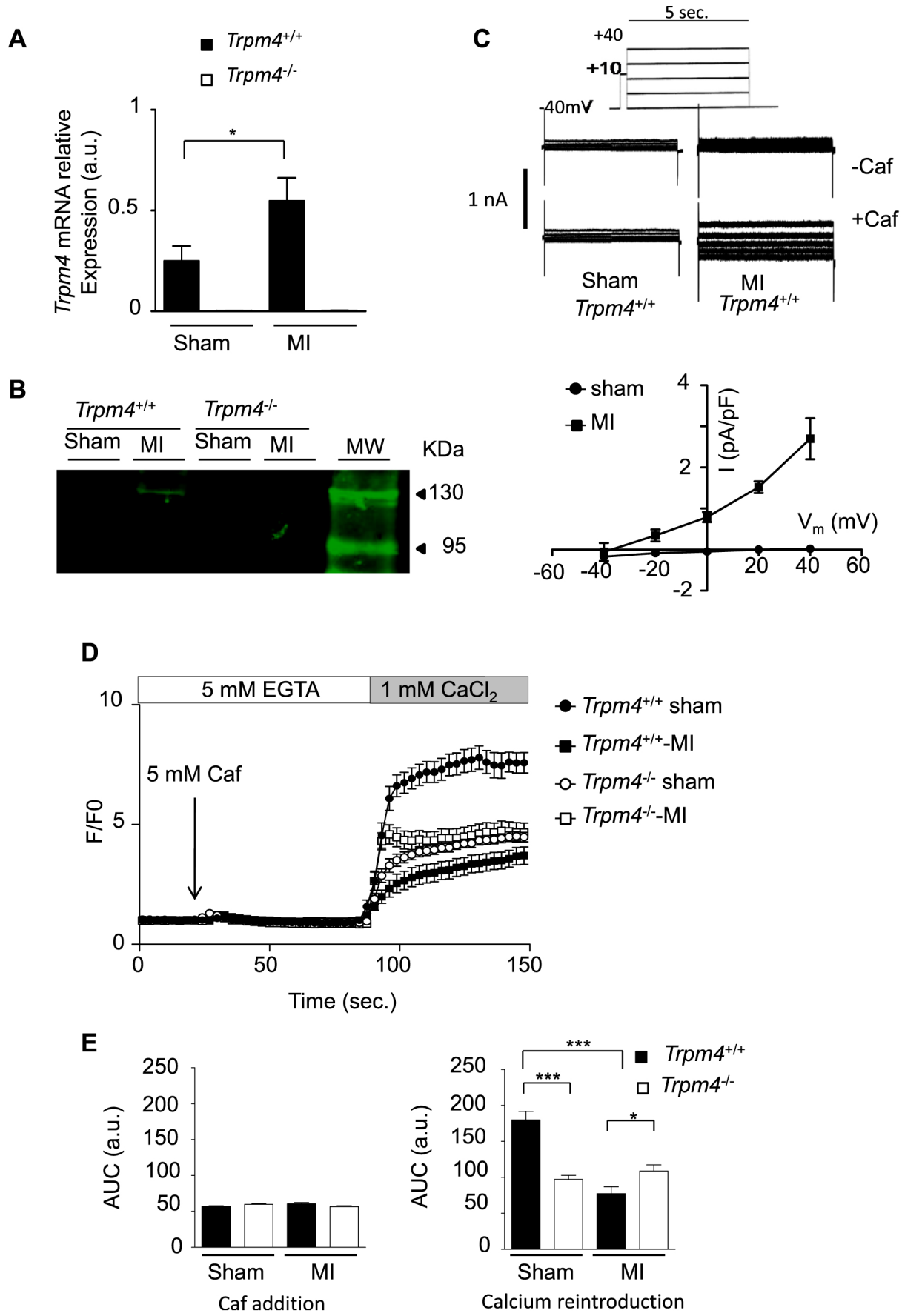
A
Trpm4+/+
Trpm4-/-
Trpm4 mRNA relative Expression (a.u.)
1
0.5
0
*
Sham
MI
B
Trpm4+/+
Trpm4-/-
Sham
MI
Sham
MI
MW
KDa
130
95
C
5 sec.
+40
+10
-40mV
1 nA
-Caf
+Caf
Sham
Trpm4+/+
MI
Trpm4+/+
sham
MI
I (pA/pF)
Vm (mV)
4
2
-2
-60
-40
-20
20
40
60
D
5 mM EGTA
1 mM CaCl2
5 mM Caf
F/F0
10
5
0
0
50
100
150
Time (sec.)
Trpm4+/+ sham
Trpm4+/+-MI
Trpm4-/- sham
Trpm4-/--MI
E
AUC (a.u.)
250
200
150
100
50
0
Sham
MI
Caf addition
***
***
*
Trpm4+/+
Trpm4-/-
Calcium reintroduction

application significantly reduced the Ca^{2+} transient amplitude in cardiomyocytes from MI-*Trpm4*$^{+/+}$ mice, suggesting that during systole, TRPM4 positively regulate Ca^{2+} transients (Fig. 4A–D). Because the β-adrenergic tone is increased during cardiac adaptation in response to MI in order to compensate for the loss of cardiac output (Triposkiadis et al., 2009), we also tested the response of cardiomyocytes to stimulation with isoprenaline (Iso, 10 nM), an adrenoreceptor (AR) agonist (Fig. 4A). As expected, Iso application induced a reduction of Ca^{2+} diastolic levels in the sham group and an increase in Ca^{2+} transient amplitude in the sham and MI groups. Moreover, 9-Phe application also lead to a decrease in Ca^{2+} transient amplitude in MI-mice.

We next investigated the effect of 9-Phe on the ECC in freshly isolated cardiomyocytes from sedentary (Sed -*Trpm4*$^{+/+}$) and trained (Tr-*Trpm4*$^{+/+}$) mice. As expected, 9-Phe had no effect on diastolic Ca^{2+} level or transient amplitude. Indeed, we have previously shown that TRPM4 is not expressed in sedentary mice (Gueffier et al., 2017) (Fig. 4B). However, since TRPM4 is functionally expressed in cardiomyocytes from trained mice, 9-Phe application had no effect on either the diastolic Ca^{2+} level or the Ca^{2+} transient amplitude. The calcium concentration appears to be too low to activate the TRPM4 channel. As β-adrenergic tone is also increased in endurance training conditions and increases calcium signals, we stimulated the adrenergic system using Iso. In these conditions, 9-Phe significantly inhibited the Iso-dependent increase of the diastolic Ca^{2+} levels and the Ca^{2+} transient amplitude (Fig. 4B).

Altogether, these data suggest a more complex role for TRPM4 than previously thought.

3.5. *Blocking TRPM4 by 9-phe significantly reduces diastolic arrhythmias*

To determine the implication of TRPM4 in arrhythmias occurring during diastole, we recorded the Ca^{2+} signal and sarcomere length (SL) under quiescent conditions (Fig. 5A). We then counted the spontaneous increase of intracellular Ca^{2+} during the unstimulated phase, associated with SL shortening in isolated cardiomyocytes from sham, MI, Sed and Tr-*Trpm4*$^{+/+}$ mice, under basal condition or following treatment with 9-Phe. Any cell which displayed one or more spontaneous Ca^{2+} increases associated with SL shortening was considered to be arrhythmic (Fig. 5B). 9-Phe application had no effect on the few arrhythmias recorded in sham and sedentary groups. However, the MI and trained groups displayed more spontaneous arrhythmias. 9-Phe application in these groups significantly decreased the number of spontaneous Ca^{2+} increases and associated arrhythmias (Fig. 5B and C). This suggests that TRPM4 is pro-arrhythmic.

4. Discussion

In this study, we provide evidence that TRPM4 is expressed in response to MI in the ventricle. In the context of MI, this expression is functional and allows for a negative regulation of SOCE as has previously been shown in other cell types such as immune cells (Barbet et al., 2008; Vennekens and Nilius, 2007) and also in cardiomyocytes from mice following endurance training (Gueffier et al., 2017). It generally accepted that SOCE is negligible in healthy, normal ventricular cardiomyocytes (Heineke and Molkentin, 2006). However, under pathological stress (increased preload or post-load), the importance of SOCE increases, mostly due to the increased expression of many other TRP channels (essentially from the TRPC subfamily) (Bush et al., 2006; Gómez et al., 2013; Guinamard and Bois, 2007; Nakayama et al., 2006; Xie et al., 2012). These channels, unlike TRPM4 which is calcium impermeable, are calcium permeable channels, and allow calcium to enter into the cell when they are open. However, this is not involved in the "contractile" calcium which regulates the calcium-induced calcium released (CICR) of the ECC (Eder and Molkentin, 2011) but rather activates other signaling pathways such as IICR (IP3R induced calcium released) (Yang et al., 2016), calcineurin (Kuwahara et al., 2006; Luo et al., 2012; Molkentin et al., 1998; Taigen et al., 2000; Wilkins et al., 2004), ERK (Gallo et al., 2019) or MAPK (Bageghni et al., 2018) which will amplify the "pathological" loop by inducing expression of the TRP channels themselves.

It has also been reported that TRPM4 is able to physically interact with TRPC3 (Park et al., 2008). This interaction reduces the calcium capacitive entry through the TRPC3 channel without generating ionic currents through the TRPM4 channel itself. This suggests a physical interaction between the two proteins leading to a dominant-negative effect.

The TRPM4 channel seems to be essential for negatively regulating the cellular "pathologic" pro-hypertrophic adaptations induced by pathological stress (Angiotensine II infusion, or post-myocardial adaptations for example (Guinamard et al., 2006; Kecskés et al., 2015)). Similar to previous reports after endurance training (Gueffier et al., 2017), we show here that, following MI, increased TRPM4 expression shifts the hypertrophic signaling pathways to a physiological response (Akt activation) whereas reduced TRPM4 expression shifts the hypertrophic signaling pathways to a pathological response (Calcineurin-NFAT activation).

Indeed, the absence of TRPM4 expression in knock-out mice significantly decreased the survival rate after MI. However, our result is in opposition of those obtained by Jacobs and collaborators. Indeed, they observed an increase of survival rate in *Trpm4*$^{-/-}$ mice when compared to *Trpm4*$^{+/+}$ mice who underwent a MI surgery (Jacobs et al., 2015). However, unlike us, they also observed TRPM4 channel expression and function in healthy isolated left ventricular cardiomyocytes in wild type mice and no hypertrophy due to hyperplasia. Suggesting that both Knock-out mice are somehow different (Demion et al., 2014; Jacobs et al., 2015; Mathar et al., 2014).

Moreover, freshly isolated cardiomyocytes from MI-*Trpm4*$^{-/-}$ mice display an increased occurrence of cellular arrhythmias (EADs and DADs) associated with ventricular PVC.

However, it seems that the TRPM4 channel does not only provide a beneficial effect during the ventricular remodeling. It has previously been shown that TRPM4 overexpression can induce the development of premature ventricular ectopic beats during exercise-induced β-adrenergic stress (Pironet et al., 2019). In

Fig. 2. Pathological cardiac hypertrophy leads to TRPM4 channel expression and function in *Trpm4*$^{+/+}$mice. **A.** Relative *Trpm4* expression in the left ventricle from sham-*Trpm4*$^{+/+}$ (N = 10), MI-*Trpm4*$^{+/+}$ (N = 5), sham-*Trpm4*$^{-/-}$ (N = 7) and MI- *Trpm4*$^{-/-}$ (N = 6) mice related to *Gapdh* housekeeping gene (a.u., arbitrary unit). **B.** TRPM4 protein expression from LV total lysate from Sham and PMI-*Trpm4*$^{+/+}$ and *Trpm4*$^{-/-}$ mice. **C.** Upper panel: Representative traces obtained when the voltage clamp protocol was applied before and after 5 mM caffeine application. Lower panel: I/V curve obtained after voltage clamp protocol presented in the upper panel in isolated cardiomyocytes from LV Sham- (black square, n = 4) and MI- (white square, n = 3) *Trpm4*$^{+/+}$ mice after 5 mM caffeine application. **D.** Mean fluorescence representing intracellular Ca^{2+} levels over time for SOCE recording from freshly isolated left ventricular myocytes from sham-*Trpm4*$^{+/+}$ (n = 48; N = 3), MI-*Trpm4*$^{+/+}$ (n = 14; N = 3), sham-*Trpm4*$^{-/-}$ (n = 34; N = 3) and MI- *Trpm4*$^{-/-}$ (n = 21; N = 3) mice. **E.** Mean area under the curve analysis (AUC) calculated in arbitrary units (a.u.) on 5 mM caffeine signal (left) or Ca^{2+}-back signal (right). N stands for the number of animals and n for the number of cells. Data are presented as mean ± SEM, statistical analysis were performed as mentioned in methods section *P < 0.05; ***P < 0.001.

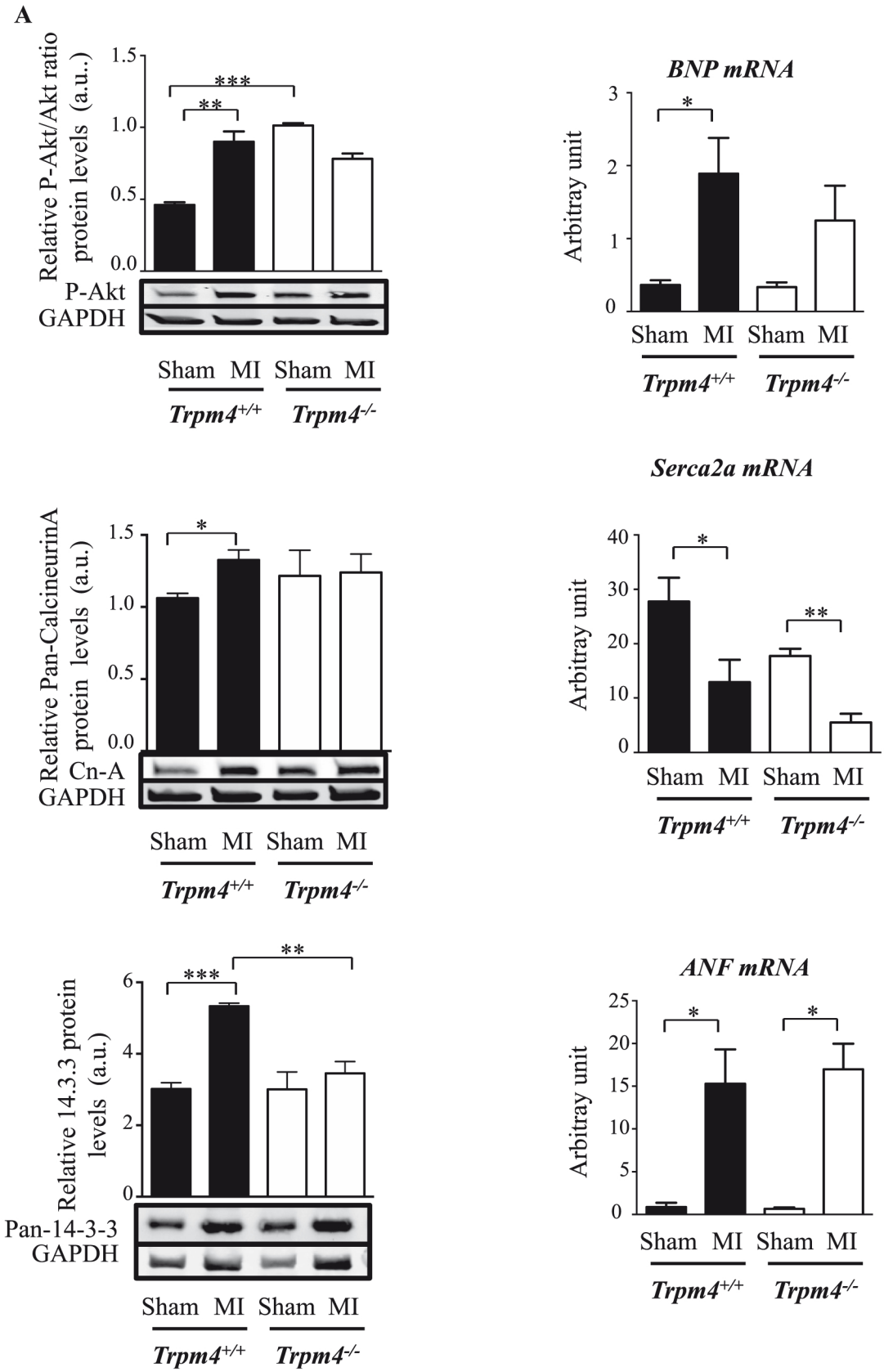

Fig. 3. Signaling pathway modulation by myocardial infarction. **A.** Relative P-Akt/Akt ratio, Pan-CnA, Pan-14.3.3, normalized to control loading GAPDH from sham-*Trpm4*$^{+/+}$ (N = 3), MI-*Trpm4*$^{+/+}$ (N = 4), sham-*Trpm4*$^{-/-}$ (N = 3) and MI- *Trpm4*$^{-/-}$ (N = 3) mice. **B.** Relative expression of *BNP, Serca2a, ANF* mRNA assessed by quantitative PCR from sham-*Trpm4*$^{+/+}$ (N = 5), MI-*Trpm4*$^{+/+}$ (N = 4), sham-*Trpm4*$^{-/-}$ (N = 3) and MI- *Trpm4*$^{-/-}$ (N = 4) mice. N stands for the number of animals. Data are presented as mean ± SEM, statistical analysis were performed as mentioned in methods section *P < 0.05; **P < 0.01; ***P < 0.001.

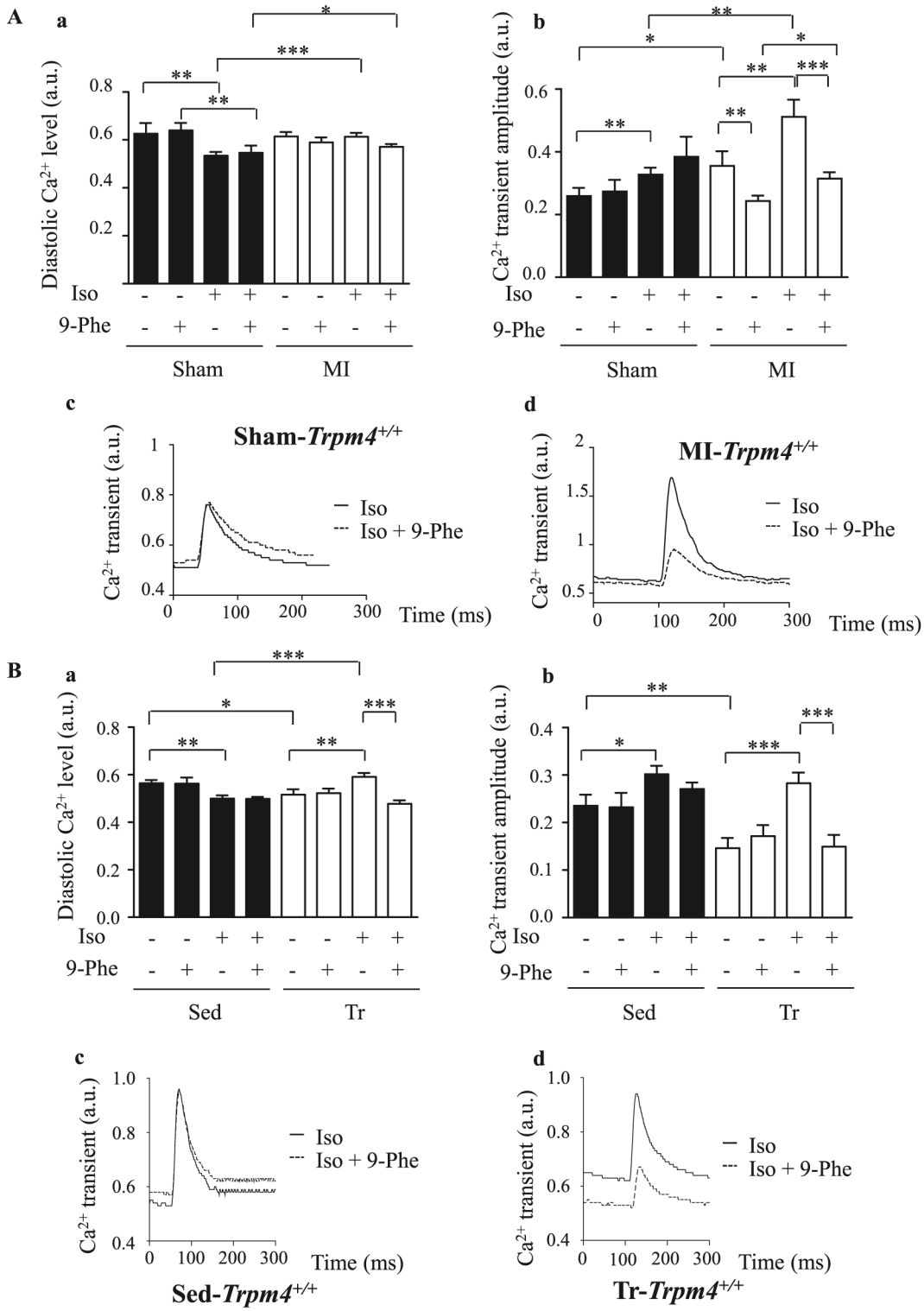

Fig. 4. Role of TRPM4 expression in calcium transient. A. Histograms representing the diastolic calcium level (a) and calcium transient amplitude (b) measured on isolated cardiomyocytes from sham (black bars) or MI mice (white bars) stimulated or not with Isoprenalin (Iso, 10 nM) and incubated or not with 9-Phe (10 μM). (c–d) Representative traces of Fura-2AM ratio obtained under Iso stimulation, incubated or not with 9-Phe (10 μM, dash line) in field-stimulated freshly isolated cardiomyocytes from sham mice (c) or MI mice (d). Cells were isolated from sham-*Trpm4*$^{+/+}$ (n = 23, 22 (9-Phe), 29 (Iso) and 26 (9-Phe + Iso) cells; N = 6), MI-*Trpm4*$^{+/+}$ (n = 30, 29 (9-Phe), 34 (Iso) and 31 (9-Phe + Iso) cells; N = 6) mice. **B.** Histograms represent the diastolic calcium level (a) and calcium transient amplitude (b) measured on isolated cardiomyocytes from sedentary (black bars) or trained mice (white bars) stimulated or not with Isoprenalin (10 nM) and incubated or not with 9-Phe (10 μM). (c–d) Representative traces of Fura-2AM ratio obtained under Iso stimulation (10 nM), incubated or not with 9-Phe (10 μM, dash line) in field-stimulated freshly isolated cardiomyocytes from sedentary (Sed) mice (c) or trained (Tr) mice (d). Cells were freshly isolated from sed-*Trpm4*$^{+/+}$ (n = 25, 13 (9-Phe), 27 (Iso) and 27 (9-Phe + Iso) cells; N = 4), MI-*Trpm4*$^{+/+}$ (n = 35, 26 (9-Phe), 23 (Iso) and 18 (9-Phe + Iso) cells; N = 4) mice. Data are presented as mean ± SEM, statistical analysis were performed as mentioned in methods section *P < 0.05; **P < 0.01; ***P < 0.001.

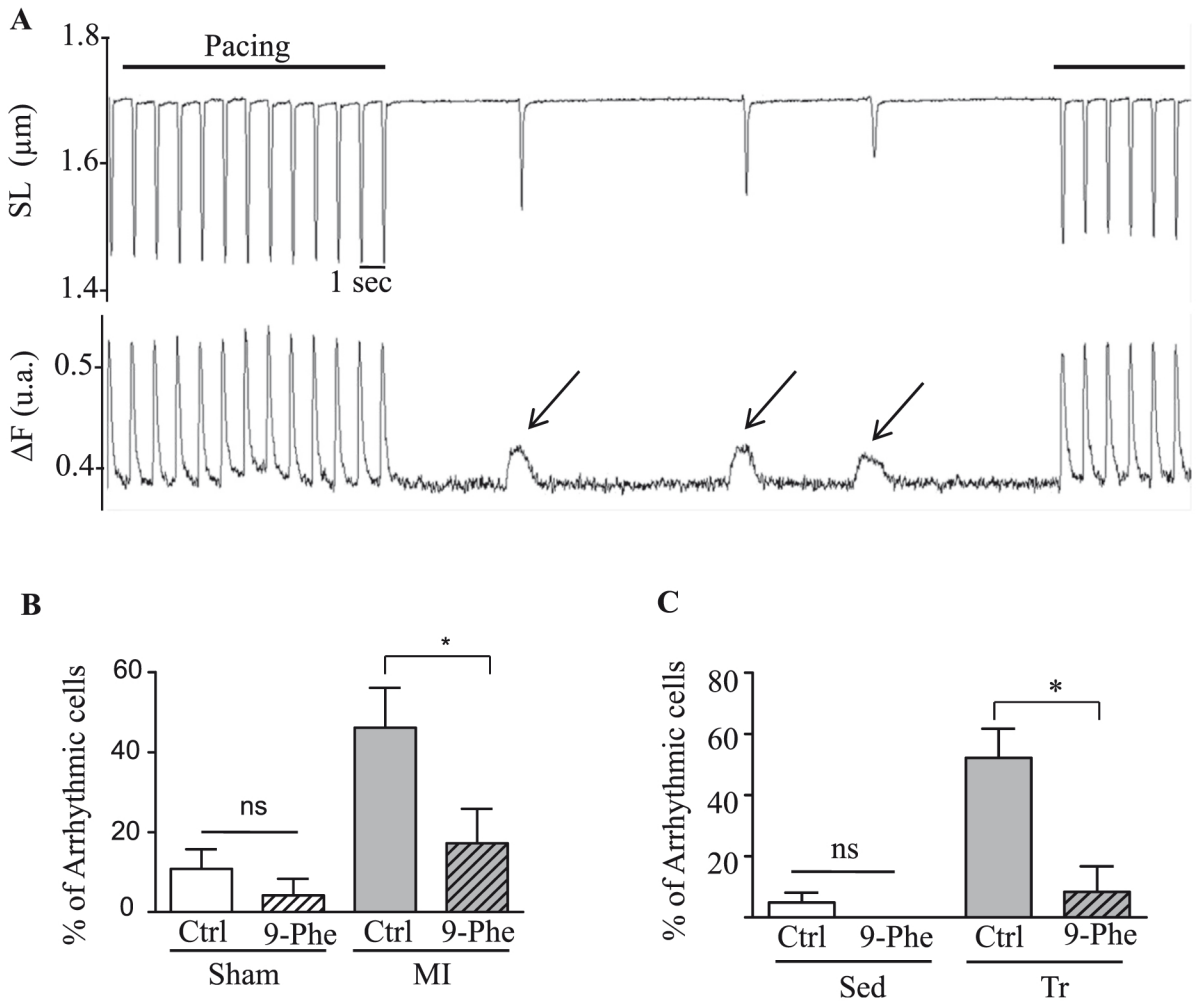

Fig. 5. Blocking TRPM4 channel significantly reduces cellular arrhythmias in both hypertrophic conditions. A. Representative sarcomere length (top) and traces of Fura-2AM ratio measurement (bottom) obtained from freshly isolated ventricular cardiomyocytes from sham or MI mice and sedentary (Sed) or trained (Tr) mice in field stimulated condition (black lines indicated pacing at 1Hz). The arrows show spontaneous rises of intracellular Ca^{2+} during diastole (unstimulated phase). **B–C.** Percentage of isolated cardiomyocytes exerting diastolic ectopic Ca^{2+} events with or without 9-Phe incubation. Cells were isolated from (B) sham-*Trpm4*$^{+/+}$ (n = 23 and 22 (9-Phe) cells; N = 6), and MI-*Trpm4*$^{+/+}$ (n = 30 and 29 (9-Phe) cells; N = 6) mice and (C) from sed-*Trpm4*$^{+/+}$ (n = 25 and 13 (9-Phe) cells; N = 4) and Tr-*Trpm4*$^{+/+}$ (n = 35 and 26 (9-Phe) cells; N = 4) mice. Data are presented as mean ± SEM, statistical analysis were performed as mentioned in methods section *P < 0.05.

patients, *TRPM4* gene mutations leading to a gain-of-function also induce conduction troubles (Kruse and Pongs, 2014; Kruse et al., 2009; Liu et al., 2010). Here, we demonstrated that, in the context of two different cellular hypertrophic remodeling, one physiological in response to endurance training and one pathological induced by myocardial infarction, cellular arrhythmias are significantly reduced by the TRPM4 channel inhibitor, 9-Phe. This result suggests that the TRPM4 channel is directly or indirectly responsible of the triggering of such arrhythmias. Conversely, it was demonstrated that 9-Phe was cardioprotective on isolated Langendorff-perfused rat hearts subjected to global ischemia and followed by reperfusion(Wang et al., 2013).

Many years ago, a calcium-activated non-selective cationic current (NSC_{Ca} or CNRS) was found to be partially responsible of the pro-arrhythmic Iti current in multiple cardiac preparations (Colquhoun et al., 1981; Guinamard et al., 2002, 2004, 2006). Indeed, spontaneous release of calcium is believed to generate a transient inward current which is arrhythmogenic. Among the numerous conductances present at the plasma membrane, the 3 most probable candidates are: a calcium-activated chloride current, an electrogenic activation of the Na^+/Ca^{2+} exchange (NCX) and a non-selective cation current (I*ns* or I*CNRS* or I*NSCca*) (Cannell et al., 1986; Fedida et al., 1987; Lipp and Pott, 1988; Matsuura and Shattock, 1991; Tsien et al., 1978; Zygmunt et al., 1998).

It is now established that NSC_{Ca} is carried by the TRPM4 channel (Demion et al., 2007). Therefore, the TRPM4 channel, when open, participates to the Iti current and is then able to trigger arrhythmias. During cardiac remodeling induced by pathological conditions, the cytosolic basal calcium concentration tends to increase. The sources of this calcium are multiple: the leaky state of the ryanodine receptor, the decreased expression of the sarco-endoplasmic reticulum ATPase (SERCA) or the increase of the NCX (Bers, 2014; Bers et al., 2002; Frank et al., 2002; Pogwizd and Bers, 2002; Stammers et al., 2015). As the TRPM4 channel is calcium activated, during diastole, Na^+ ions enter into the cell, participating to the Iti current.

The more surprising results come from the effect of 9-Phe on Ca^{2+} transient amplitude. The TRPM4 channel inhibition induced a decreased amplitude in cardiomyocytes from MI-*Trpm4*$^{+/+}$ mice. Since TRPM4 is known to negatively regulate SOCE, the positive regulation of Ca^{2+} transient amplitude, not observed in sham-*Trpm4*$^{+/+}$ mice, is intriguing. As reported before (Bers et al., 2002),

the ventricular remodeling induced by MI includes the increase of NCX expression. In a very recent study, Cantero-Recasens et al. have demonstrated that the TRPM4 channel and the NCX are able to cooperate to control Ca^{2+} signal in bronchial epithelial cells (Cantero-Recasens et al., 2019). The proposed mechanism is the following: Na^{+} ions enter by the TRPM4 channel and are then extruded by NCX which in turn allows Ca^{2+} ions to enter. Our results are in line with this hypothesis. Indeed, in freshly isolated ventricular cardiomyocytes from Tr-*Trpm4*$^{+/+}$, 9-Phe has no effect on Ca^{2+} transient amplitude, but when stimulated with an adrenergic agonist, 9-Phe significantly reduces the Ca^{2+} transient amplitude. In this type of remodeling, we have previously published that the SERCA expression is increased (Gueffier et al., 2017). Therefore, in normal conditions, diastolic Ca^{2+} concentration is perfectly regulated and is not high enough to activate the TRPM4 channel. However, during Iso stimulation, the diastolic Ca^{2+} concentration increases, activates the TRPM4 channel and this could allow the NCX to work, amplifying the Ca^{2+} transient.

Other data comforting this hypothesis come from the fact that the activity of NCX is increased by the Protein Kinase A (Zhang and Hancox, 2009; Pulina et al., 2006; Ruknudin et al., 2007). In β-adrenergic stimulation, NCX activity is also likely enhanced by itself in response to protein Kinase A activation.

These results are also in line with those obtained recently (Pironet et al., 2019) with the TRPM4 channel overexpression mouse model, which develops premature ventricular ectopic beats during exercise-induced β-adrenergic stress.

Limitations of the study: Since our MI-*Trpm4*$^{-/-}$ animals showed a survival rate of 50%, we could only conduct our study on a low number of animals, which could potentially exert a different phenotype from those who died. Although this could induce a bias in our work, here we only focused on living animals and it would be interesting to perform autopsy on the dead ones to know whether their hearts display a similar phenotype or not.

Because of the afore-mentioned survival rate and the fact that we worked with littermate, some of our experiments, in particular Western blot analysis or qPCR, were perform with a relatively low N number. Although this brings a limitation of our study and could benefit from expended number of samples, our results were statistically significant due to weak variability and comforts our hypothesis that the lack of TRPM4 expression alters the pro-hypertrophic signaling pathways. Finally, in our model of myocardial infarction, we observed a ventricular dilation (eccentric hypertrophy), an expected consequence of a permanent occlusion(Iismaa et al., 2018). In particular, we observed cellular hypertrophy of isolated cardiomyocytes in the periinfarct area. In the endurance training model, we also observed hypertrophy which was in this case reflected by a harmonious growth. Although, our study did not focus on all types of hypertrophies (concentric and/or eccentric and/or harmonious), our results show that TRPM4 plays a role in establishing hypertrophic signaling pathways (pathological or physiological).

In summary, this study shows for the first time that TRPM4 channel expression is not good or bad, but more likely both, acting to shift the cellular hypertrophic signaling pathways from pathological to physiological, but also probably participating to the Iti current in cooperation with the NCX to generate cellular arrhythmias.

Author contributions

MD designed experiments with input from SR, JYL and KL.

CH, KL and NC performed the experiments such as training, excitation-contraction coupling experiments.

JT performed the ECG experiments and analysis.

CC performed the echocardiographic experiments and analysis.

FA performed cardiomyocytes isolation and AP measurements.

PB performed the surgery on MI and sham groups.

MD performed electrophysiological, RT-qPCR, SOCE, Western-blot experiments.

MD, JYL and AF wrote the manuscript with input from KL and JT.

Funding sources

This work was supported by the *Agence Nationale de la Recherche* ("Target channel"; RPV09046FSA; "Beat-genesis" 2010 blanc 1128 03), *Région Languedoc-Roussillon* (*GEPETOS*), grants from the *Université Montpellier 2* and the *Fondation de France* (Synaptocard project, N°2013–00038586).

Acknowledgments

Echocardiography were performed on the *Plateforme Imagerie du Petit Animal de Montpellier* (IPAM; http://www.ipam.cnrs.fr).

References

Abriel, H., Syam, N., Sottas, V., Amarouch, M.Y., Rougier, J.-S., 2012. TRPM4 channels in the cardiovascular system: physiology, pathophysiology, and pharmacology. Biochem. Pharmacol. 84, 873–881.

Bageghni, S.A., Hemmings, K.E., Zava, N., Denton, C.P., Porter, K.E., Ainscough, J.F.X., Drinkhill, M.J., Turner, N.A., 2018. Cardiac fibroblast-specific p38α MAP kinase promotes cardiac hypertrophy via a putative paracrine interleukin-6 signaling mechanism. FASEB J. Off. Publ. Fed. Am. Soc. Exp. Biol. 32, 4941–4954.

Barbet, G., Demion, M., Moura, I.C., Serafini, N., Léger, T., Vrtovsnik, F., Monteiro, R.C., Guinamard, R., Kinet, J.-P., Launay, P., 2008. The calcium-activated nonselective cation channel TRPM4 is essential for the migration but not the maturation of dendritic cells. Nat. Immunol. 9, 1148–1156.

Bers, D.M., 2014. Cardiac sarcoplasmic reticulum calcium leak: basis and roles in cardiac dysfunction. Annu. Rev. Physiol. 76, 107–127.

Bers, D.M., Pogwizd, S.M., Schlotthauer, K., 2002. Upregulated Na/Ca exchange is involved in both contractile dysfunction and arrhythmogenesis in heart failure. Basic Res. Cardiol. 97 (Suppl. 1), I36–I42.

Bush, E.W., Hood, D.B., Papst, P.J., Chapo, J.A., Minobe, W., Bristow, M.R., Olson, E.N., McKinsey, T.A., 2006. Canonical transient receptor potential channels promote cardiomyocyte hypertrophy through activation of calcineurin signaling. J. Biol. Chem. 281, 33487–33496.

Cannell, M.B., Eisner, D.A., Lederer, W.J., Valdeolmillos, M., 1986. Effects of membrane potential on intracellular calcium concentration in sheep Purkinje fibres in sodium-free solutions. J. Physiol. 381, 193–203.

Cantero-Recasens, G., Butnaru, C.M., Brouwers, N., Mitrovic, S., Valverde, M.A., Malhotra, V., 2019. Sodium channel TRPM4 and sodium/calcium exchangers (NCX) cooperate in the control of Ca2+-induced mucin secretion from goblet cells. J. Biol. Chem. 294, 816–826.

Colquhoun, D., Neher, E., Reuter, H., Stevens, C.F., 1981. Inward current channels activated by intracellular Ca in cultured cardiac cells. Nature 294, 752–754.

Dai, W., Bai, Y., Hebda, L., Zhong, X., Liu, J., Kao, J., Duan, C., 2014. Calcium deficiency-induced and TRP channel-regulated IGF1R-PI3K-Akt signaling regulates abnormal epithelial cell proliferation. Cell Death Differ. 21, 568–581.

DeBosch, B., Treskov, I., Lupu, T.S., Weinheimer, C., Kovacs, A., Courtois, M., Muslin, A.J., 2006. Akt 1 is required for physiological cardiac growth. Circulation 113, 2097–2104.

Demion, M., Bois, P., Launay, P., Guinamard, R., 2007. TRPM4, a Ca2+-activated nonselective cation channel in mouse sino-atrial node cells. Cardiovasc. Res. 73, 531–538.

Demion, M., Thireau, J., Gueffier, M., Finan, A., Khoueiry, Z., Cassan, C., Serafini, N., Aimond, F., Granier, M., Pasquié, J.-L., et al., 2014. Trpm4 gene invalidation leads to cardiac hypertrophy and electrophysiological alterations. PloS One 9, e115256.

Duthoit, G., Fressart, V., Hidden-Lucet, F., Simon, F., Kattygnarath, D., Charron, P., Himbert, C., Aouate, P., Guicheney, P., Lecarpentier, Y., et al., 2012. Brugada ECG pattern: a physiopathological prospective study based on clinical, electrophysiological, angiographic, and genetic findings. Front. Physiol. 3, 474.

Eder, P., Molkentin, J.D., 2011. TRPC channels as effectors of cardiac hypertrophy. Circ. Res. 108, 265–272.

Fauconnier, J., Pasquié, J.-L., Bideaux, P., Lacampagne, A., Richard, S., 2010. Cardiomyocytes hypertrophic status after myocardial infarction determines distinct types of arrhythmia: role of the ryanodine receptor. Prog. Biophys. Mol.

Biol. 103, 71–80.
Fedida, D., Noble, D., Rankin, A.C., Spindler, A.J., 1987. The arrhythmogenic transient inward current iTI and related contraction in isolated Guinea-pig ventricular myocytes. J. Physiol. 392, 523–542.
Frank, K.F., Bölck, B., Brixius, K., Kranias, E.G., Schwinger, R.H.G., 2002. Modulation of SERCA: implications for the failing human heart. Basic Res. Cardiol. 97 (Suppl. 1), I72–I78.
Gallo, S., Vitacolonna, A., Bonzano, A., Comoglio, P., Crepaldi, T., 2019. ERK: a key player in the pathophysiology of cardiac hypertrophy. Int. J. Mol. Sci. 20.
Gómez, A.M., Ruiz-Hurtado, G., Benitah, J.-P., Domínguez-Rodríguez, A., 2013. Ca(2+) fluxes involvement in gene expression during cardiac hypertrophy. Curr. Vasc. Pharmacol. 11, 497–506.
Gueffier, M., Zintz, J., Lambert, K., Finan, A., Aimond, F., Chakouri, N., Hédon, C., Granier, M., Launay, P., Thireau, J., et al., 2017. The TRPM4 channel is functionally important for the beneficial cardiac remodeling induced by endurance training. J. Muscle Res. Cell Motil. 38, 3–16.
Guinamard, R., Bois, P., 2007. Involvement of transient receptor potential proteins in cardiac hypertrophy. Biochim. Biophys. Acta 1772, 885–894.
Guinamard, R., Rahmati, M., Lenfant, J., Bois, P., 2002. Characterization of a Ca2+-activated nonselective cation channel during dedifferentiation of cultured rat ventricular cardiomyocytes. J. Membr. Biol. 188, 127–135.
Guinamard, R., Chatelier, A., Demion, M., Potreau, D., Patri, S., Rahmati, M., Bois, P., 2004. Functional characterization of a Ca(2+)-activated non-selective cation channel in human atrial cardiomyocytes. J. Physiol. 558, 75–83.
Guinamard, R., Demion, M., Chatelier, A., Bois, P., 2006a. Calcium-activated nonselective cation channels in mammalian cardiomyocytes. Trends Cardiovasc. Med. 16, 245–250.
Guinamard, R., Demion, M., Magaud, C., Potreau, D., Bois, P., 2006b. Functional expression of the TRPM4 cationic current in ventricular cardiomyocytes from spontaneously hypertensive rats. Hypertension 48, 587–594.
Guinamard, R., Hof, T., Sallé, L., 2014. Current recordings at the single channel level in adult mammalian isolated cardiomyocytes. Methods Mol. Biol. Clifton NJ 1183, 291–307.
Heineke, J., Molkentin, J.D., 2006. Regulation of cardiac hypertrophy by intracellular signalling pathways. Nat. Rev. Mol. Cell Biol. 7, 589–600.
Hof, T., Simard, C., Rouet, R., Sallé, L., Guinamard, R., 2013. Implication of the TRPM4 nonselective cation channel in mammalian sinus rhythm. Heart Rhythm off. J. Heart Rhythm Soc. 10, 1683–1689.
Hu, Y., Duan, Y., Takeuchi, A., Hai-Kurahara, L., Ichikawa, J., Hiraishi, K., Numata, T., Ohara, H., Iribe, G., Nakaya, M., et al., 2017. Uncovering the arrhythmogenic potential of TRPM4 activation in atrial-derived HL-1 cells using novel recording and numerical approaches. Cardiovasc. Res. 113, 1243–1255.
Iismaa, S.E., Li, M., Kesteven, S., Wu, J., Chan, A.Y., Holman, S.R., Calvert, J.W., Haq, A.U., Nicks, A.M., Naqvi, N., et al., 2018. Cardiac hypertrophy limits infarct expansion after myocardial infarction in mice. Sci. Rep. 8, 6114.
Jacobs, G., Oosterlinck, W., Dresselaers, T., Geenens, R., Kerselaers, S., Himmelreich, U., Herijgers, P., Vennekens, R., 2015. Enhanced β-adrenergic cardiac reserve in Trpm4$^{-/-}$ mice with ischaemic heart failure. Cardiovasc. Res. 105, 330–339.
Kecskés, M., Jacobs, G., Kerselaers, S., Syam, N., Menigoz, A., Vangheluwe, P., Freichel, M., Flockerzi, V., Voets, T., Vennekens, R., 2015. The Ca(2+)-activated cation channel TRPM4 is a negative regulator of angiotensin II-induced cardiac hypertrophy. Basic Res. Cardiol. 110, 43.
Kemi, O.J., Ceci, M., Wisloff, U., Grimaldi, S., Gallo, P., Smith, G.L., Condorelli, G., Ellingsen, O., 2008. Activation or inactivation of cardiac Akt/mTOR signaling diverges physiological from pathological hypertrophy. J. Cell. Physiol. 214, 316–321.
Kim, J., Wende, A.R., Sena, S., Theobald, H.A., Soto, J., Sloan, C., Wayment, B.E., Litwin, S.E., Holzenberger, M., LeRoith, D., et al., 2008. Insulin-like growth factor I receptor signaling is required for exercise-induced cardiac hypertrophy. Mol. Endocrinol. Baltim. Md 22, 2531–2543.
Köster, O.F., Szigeti, G.P., Beuckelmann, D.J., 1999. Characterization of a [Ca2+]i-dependent current in human atrial and ventricular cardiomyocytes in the absence of Na+ and K+. Cardiovasc. Res. 41, 175–187.
Kruse, M., Pongs, O., 2014. TRPM4 channels in the cardiovascular system. Curr. Opin. Pharmacol. 15, 68–73.
Kruse, M., Schulze-Bahr, E., Corfield, V., Beckmann, A., Stallmeyer, B., Kurtbay, G., Ohmert, I., Schulze-Bahr, E., Brink, P., Pongs, O., 2009. Impaired endocytosis of the ion channel TRPM4 is associated with human progressive familial heart block type I. J. Clin. Invest. 119, 2737–2744.
Kuwahara, K., Wang, Y., McAnally, J., Richardson, J.A., Bassel-Duby, R., Hill, J.A., Olson, E.N., 2006. TRPC6 fulfills a calcineurin signaling circuit during pathologic cardiac remodeling. J. Clin. Invest. 116, 3114–3126.
Lee, K.S., Tsien, R.W., 1984. High selectivity of calcium channels in single dialysed heart cells of the Guinea-pig. J. Physiol. 354, 253–272.
Lipp, P., Pott, L., 1988. Transient inward current in Guinea-pig atrial myocytes reflects a change of sodium-calcium exchange current. J. Physiol. 397, 601–630.
Liu, H., El Zein, L., Kruse, M., Guinamard, R., Beckmann, A., Bozio, A., Kurtbay, G., Mégarbané, A., Ohmert, I., Blaysat, G., et al., 2010. Gain-of-function mutations in TRPM4 cause autosomal dominant isolated cardiac conduction disease. Circ. Cardiovasc. Genet. 3, 374–385.
Liu, H., Chatel, S., Simard, C., Syam, N., Salle, L., Probst, V., Morel, J., Millat, G., Lopez, M., Abriel, H., et al., 2013. Molecular genetics and functional anomalies in a series of 248 Brugada cases with 11 mutations in the TRPM4 channel. PloS One 8, e54131.
Luo, X., Hojayev, B., Jiang, N., Wang, Z.V., Tandan, S., Rakalin, A., Rothermel, B.A., Gillette, T.G., Hill, J.A., 2012. STIM1-dependent store-operated Ca^{2+} entry is required for pathological cardiac hypertrophy. J. Mol. Cell. Cardiol. 52, 136–147.
Martin, V.A., Wang, W.-H., Lipchik, A.M., Parker, L.L., He, Y., Zhang, S., Zhang, Z.-Y., Geahlen, R.L., 2012. Akt 2 inhibits the activation of NFAT in lymphocytes by modulating calcium release from intracellular stores. Cell. Signal. 24, 1064–1073.
Mathar, I., Vennekens, R., Meissner, M., Kees, F., Van der Mieren, G., Camacho Londoño, J.E., Uhl, S., Voets, T., Hummel, B., van den Bergh, A., et al., 2010. Increased catecholamine secretion contributes to hypertension in TRPM4-deficient mice. J. Clin. Invest. 120, 3267–3279.
Mathar, I., Kecskes, M., Van der Mieren, G., Jacobs, G., Camacho Londoño, J.E., Uhl, S., Flockerzi, V., Voets, T., Freichel, M., Nilius, B., et al., 2014. Increased β-adrenergic inotropy in ventricular myocardium from Trpm4-/- mice. Circ. Res. 114, 283–294.
Matsui, T., Nagoshi, T., Rosenzweig, A., 2003. Akt and PI 3-kinase signaling in cardiomyocyte hypertrophy and survival. Cell Cycle Georget. Tex 2, 220–223.
Matsuura, H., Shattock, M.J., 1991. Membrane potential fluctuations and transient inward currents induced by reactive oxygen intermediates in isolated rabbit ventricular cells. Circ. Res. 68, 319–329.
Molkentin, J.D., Lu, J.R., Antos, C.L., Markham, B., Richardson, J., Robbins, J., Grant, S.R., Olson, E.N., 1998. A calcineurin-dependent transcriptional pathway for cardiac hypertrophy. Cell 93, 215–228.
Nakayama, H., Wilkin, B.J., Bodi, I., Molkentin, J.D., 2006. Calcineurin-dependent cardiomyopathy is activated by TRPC in the adult mouse heart. FASEB J. Off. Publ. Fed. Am. Soc. Exp. Biol. 20, 1660–1670.
Nilius, B., Prenen, J., Janssens, A., Owsianik, G., Wang, C., Zhu, M.X., Voets, T., 2005. The selectivity filter of the cation channel TRPM4. J. Biol. Chem. 280, 22899–22906.
Oliveira, R.S.F., Ferreira, J.C.B., Gomes, E.R.M., Paixão, N.A., Rolim, N.P.L., Medeiros, A., Guatimosim, S., Brum, P.C., 2009. Cardiac anti-remodelling effect of aerobic training is associated with a reduction in the calcineurin/NFAT signalling pathway in heart failure mice. J. Physiol. 587, 3899–3910.
Park, J.-Y., Hwang, E.M., Yarishkin, O., Seo, J.-H., Kim, E., Yoo, J., Yi, G.-S., Kim, D.-G., Park, N., Ha, C.M., et al., 2008. TRPM4b channel suppresses store-operated Ca2+ entry by a novel protein-protein interaction with the TRPC3 channel. Biochem. Biophys. Res. Commun. 368, 677–683.
Pironet, A., Syam, N., Vandewiele, F., Van den Haute, C., Kerselaers, S., Pinto, S., Vande Velde, G., Gijsbers, R., Vennekens, R., 2019. AAV9-Mediated overexpression of TRPM4 increases the incidence of stress-induced ventricular arrhythmias in mice. Front. Physiol. 10, 802.
Pogwizd, S.M., Bers, D.M., 2002. Calcium cycling in heart failure: the arrhythmia connection. J. Cardiovasc. Electrophysiol. 13, 88–91.
Pulina, M.V., Rizzuto, R., Brini, M., Carafoli, E., 2006. Inhibitory interaction of the plasma membrane Na+/Ca2+ exchangers with the 14-3-3 proteins. J. Biol. Chem. 281, 19645–19654.
Ruknudin, A.M., Wei, S.-K., Haigney, M.C., Lederer, W.J., Schulze, D.H., 2007. Phosphorylation and other conundrums of Na/Ca exchanger, NCX1. Ann. N. Y. Acad. Sci. 1099, 103–118.
Simard, C., Sallé, L., Rouet, R., Guinamard, R., 2012. Transient receptor potential melastatin 4 inhibitor 9-phenanthrol abolishes arrhythmias induced by hypoxia and re-oxygenation in mouse ventricle. Br. J. Pharmacol. 165, 2354–2364.
Simard, C., Hof, T., Keddache, Z., Launay, P., Guinamard, R., 2013. The TRPM4 nonselective cation channel contributes to the mammalian atrial action potential. J. Mol. Cell. Cardiol. 59, 11–19.
Stallmeyer, B., Zumhagen, S., Denjoy, I., Duthoit, G., Hébert, J.-L., Ferrer, X., Maugenre, S., Schmitz, W., Kirchhefer, U., Schulze-Bahr, E., et al., 2012. Mutational spectrum in the Ca(2+)–activated cation channel gene TRPM4 in patients with cardiac conductance disturbances. Hum. Mutat. 33, 109–117.
Stammers, A.N., Susser, S.E., Hamm, N.C., Hlynsky, M.W., Kimber, D.E., Kehler, D.S., Duhamel, T.A., 2015. The regulation of sarco(endo)plasmic reticulum calcium-ATPases (SERCA). Can. J. Physiol. Pharmacol. 93, 843–854.
Taigen, T., De Windt, L.J., Lim, H.W., Molkentin, J.D., 2000. Targeted inhibition of calcineurin prevents agonist-induced cardiomyocyte hypertrophy. Proc. Natl. Acad. Sci. U.S.A. 97, 1196–1201.
Triposkiadis, F., Karayannis, G., Giamouzis, G., Skoularigis, J., Louridas, G., Butler, J., 2009. The sympathetic nervous system in heart failure physiology, pathophysiology, and clinical implications. J. Am. Coll. Cardiol. 54, 1747–1762.
Tsien, R.W., Kass, R.S., Weingart, R., 1978. Calcium ions and membrane current changes induced by digitals in cardiac Purkinje fibers. Ann. N. Y. Acad. Sci. 307, 483–490.
Uhl, S., Mathar, I., Vennekens, R., Freichel, M., 2014. Adenylyl cyclase-mediated effects contribute to increased Isoprenaline-induced cardiac contractility in TRPM4-deficient mice. J. Mol. Cell. Cardiol. 74, 307–317. https://doi.org/10.1016/j.yjmcc.2014.06.007.
Vennekens, R., Nilius, B., 2007. Insights into TRPM4 function, regulation and physiological role. Handb. Exp. Pharmacol. 269–285.
Wang, J., Takahashi, K., Piao, H., Qu, P., Naruse, K., 2013. 9-Phenanthrol, a TRPM4 inhibitor, protects isolated rat hearts from ischemia-reperfusion injury. PloS One 8, e70587.
Wilkins, B.J., Dai, Y.-S., Bueno, O.F., Parsons, S.A., Xu, J., Plank, D.M., Jones, F., Kimball, T.R., Molkentin, J.D., 2004. Calcineurin/NFAT coupling participates in pathological, but not physiological, cardiac hypertrophy. Circ. Res. 94, 110–118.
Xie, J., Cha, S.-K., An, S.-W., Kuro-O, M., Birnbaumer, L., Huang, C.-L., 2012. Cardioprotection by Klotho through downregulation of TRPC6 channels in the

mouse heart. Nat. Commun. 3, 1238.
Yang, Y., Zhou, Y., Cao, Z., Tong, X.Z., Xie, H.Q., Luo, T., Hua, X.P., Wang, H.Q., 2016. miR-155 functions downstream of angiotensin II receptor subtype 1 and calcineurin to regulate cardiac hypertrophy. Exp. Ther. Med. 12, 1556–1562.
Zhang, Y.H., Hancox, J.C., 2009. Regulation of cardiac Na+-Ca2+ exchanger activity by protein kinase phosphorylation–still a paradox? Cell Calcium 45, 1–10.
Zygmunt, A.C., Goodrow, R.J., Weigel, C.M., 1998. INaCa and ICl(Ca) contribute to isoproterenol-induced delayed after depolarizations in midmyocardial cells. Am. J. Physiol. 275, H1979–H1992.